



0960-894X(95)00311-8

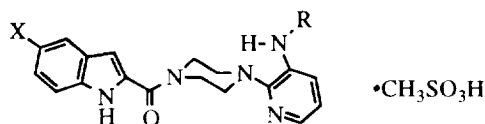
DESIGN AND SYNTHESIS OF A CONFORMATIONALLY CONSTRAINED ANALOG OF THE BIS(HETEROARYL)PIPERAZINE (BHAP) HIV-1 REVERSE TRANSCRIPTASE INHIBITOR ATEVIRDINE

Michael J. Genin^a, Constance G. Chidester^b, Douglas C. Rohrer^c, and Donna L. Romero^{a*}

^aMedicinal Chemistry Research, ^bPhysical and Analytical Chemistry, and ^cComputer-Aided Drug Design
Upjohn Laboratories, 301 Henrietta St., Kalamazoo, MI 49001

Abstract: The design and synthesis of a novel conformationally constrained spiro analog of the BHAP class of HIV-1 reverse transcriptase inhibitors, based on the molecular modeling and the X-ray crystal structure of the clinical candidate atevirdine, is described.

The discovery of the bis(heteroaryl)piperazine (BHAP) class of HIV-1 reverse transcriptase (HIV-1 RT) inhibitors has led to the development of the clinical candidates atevirdine mesylate and delavirdine mesylate.¹⁻⁴ Both of these compounds are potent inhibitors of HIV-1 RT and show promise for the treatment of HIV infection. Recently, we have been interested in probing the biologically active conformation of these molecules so that we might be able to design analogs with enhanced activity and/or metabolic stability.



	X	R	RT inhibition <i>in vitro</i>		Inhibition of viral replication (PBMC), ED ₅₀ (μM)
			% (100 μM)	IC ₅₀ (μM)	
Atevirdine	-OCH ₃	-Et	92	5.2	0.001
Delavirdine	-NHSO ₂ Me	- <i>i</i> -Pr	98	1.1	0.0001

Accurate conformational analyses of BHAP structures required the availability of suitable molecular mechanics parameters. Substructure searches of the Cambridge Crystallographic Database⁵ were conducted in order to determine the structural characteristics of the various portions of the BHAP molecule, especially the piperazine ring and substituent conformational preferences, for use in parameter development. These data revealed that the piperazine ring preferred a chair conformation with the amide-piperazine nitrogen planar and the pyridine-piperazine nitrogen tetrahedral. Once the molecular mechanics potentials were adjusted to accurately predict these results, systematic conformational searches of the four rotatable bonds were performed on a BHAP prototype^{6,7} with the pyridine ring bonded to the piperazine in either the axial or equatorial position. The preferred energy minimized conformation of the BHAP (**Figure 1**) had the pyridine-ring bond equatorial to the piperazine with its ring plane nearly perpendicular to the piperazine ring and the 3-alkylamino side-chain on the side opposite the nearest axial protons. These orientations apparently minimize steric interactions.



Figure 1. Minimum energy conformation of a BHAP prototype.

The X-ray crystal structures of atevirdine (**Figure 2**) and atevirdine hydrochloride have been solved⁸ and the results confirm the molecular modeling analysis discussed above. In the solid state, these BHAP molecules adopt an extended conformation with the piperazine linker existing in a chair conformation and the pyridine equatorial with respect to the piperazine. However, one unique feature observed in both crystal structures was an intramolecular hydrogen bond between the 3-(ethylamino)pyridinyl hydrogen and the lone pair of the piperazine nitrogen attached to the 2-position of the pyridine ring. The N-N distances were 2.71(1)Å for atevirdine and 2.80(1)Å for atevirdine hydrochloride. We hypothesized that this hydrogen bonded ground state conformation may also be the biologically active conformation of the BHAPs. To test this hypothesis, we designed the constrained analog **1**, wherein the five-membered spiro ring system acts as a permanent conformational lock in place of the intramolecular hydrogen bond.

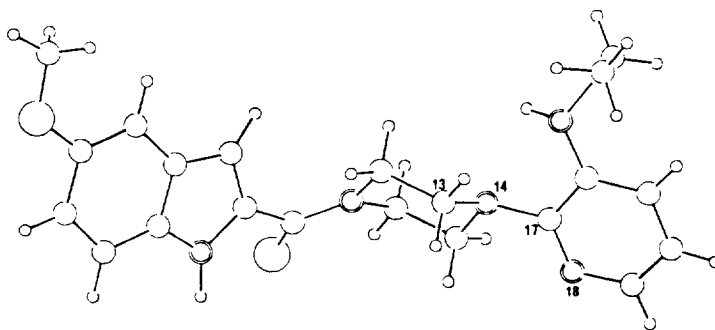
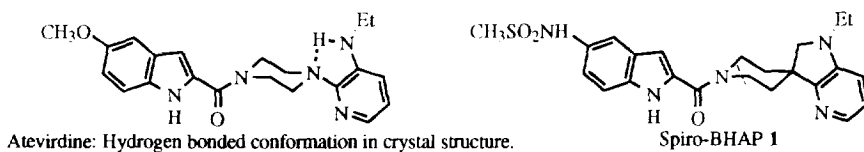


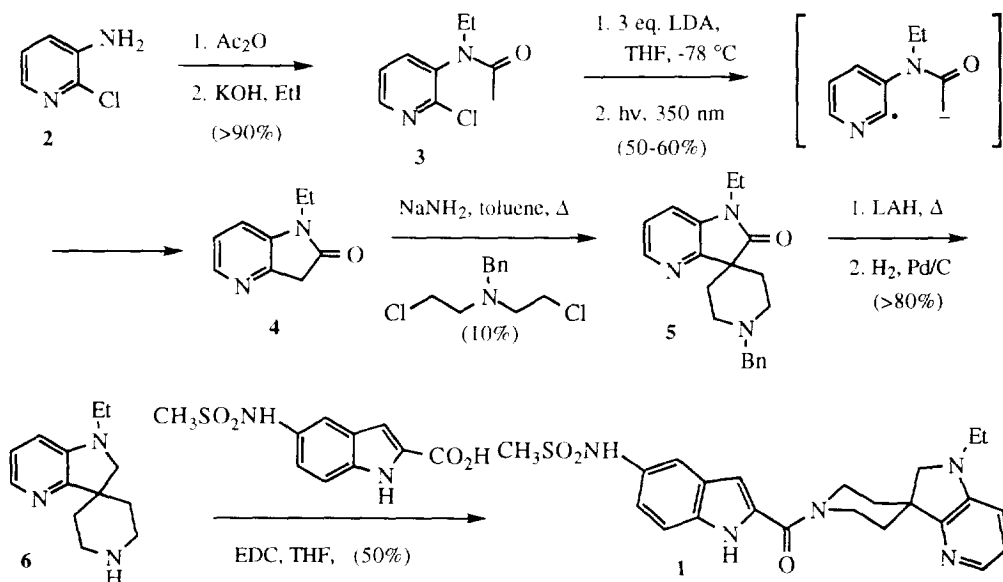
Figure 2. X-ray crystal structure of atevirdine.



SYNTHESIS

The key intermediate in the synthesis of the targeted spiro-BHAP is the novel spiro system **6** (Scheme 1). While the synthesis of spiroindolines is precededented,^{9,10} the synthesis of analogous spiroazaindolines is not. Thus, the route we embarked upon began with the acylation of 2-chloro-3-aminopyridine, **2**, followed by alkylation of the resulting amide to provide **3** in high yields. This material was then converted to the azaoxindole **4** via a photocatalyzed radical-anion cyclization.¹¹ This reaction proceeded very cleanly to give **4** in yields ranging from 50–60%. Following literature precedent⁹ for conversion of an oxindole into a similar spirocyclic system (~51% yield), azaoxindole **4** was treated with NaNH₂ and N-benzyl-bis-2-chloroethylamine in refluxing toluene to afford the desired 5-membered spiro system **5** in low yields (10%). Unfortunately, various combinations of bases (BuLi, NaH, KH), solvent systems (toluene, THF, DMF), and temperatures (-78 to +100 °C) led to similar or worse yields of **5**. Nevertheless, reduction of **5** followed by deprotection gave the desired spiroindoline intermediate, **6**, which was coupled to the indole-2-carboxylic acid derivative to afford the spiro-BHAP analog **1**.¹²

Scheme 1



BIOLOGICAL EVALUATION

The spiro-BHAP analog **1** was tested for its ability to inhibit HIV-1 RT¹³ *in vitro* and was found to inhibit the enzyme by 38% at 100 μ M. This compound is much less active than atevirdine (92-98% RT inhibition at 100 μ M).^{1,2,14} In the X-ray structures of atevirdine and atevirdine hydrochloride the torsion angles defined by N18-C17-N14-C13 were found to be 114.7(7)° and 129.5(4)°, respectively. This same angle was estimated to be 112° in the earlier molecular modeling study of atevirdine. Molecular modeling of spirocyclic **1**^{15,16} shows that the pyridine ring is nearly orthogonal to the plane of the piperidine ring (**Figure 3**) and that the 5-membered spiro system is highly rigid. The torsion angle defined by N18-C17-C14-C13 was estimated to be 79°. This, however, does not exactly mimic the analogous torsion angles found in atevirdine and atevirdine hydrochloride. If the relative conformation of the pyridine and piperazine moieties observed in the X-ray structure of atevirdine correspond to the biologically active conformation, then the differences in this region of spirocyclic **1** could account for the loss in RT inhibitory activity. For example, since the pyridine nitrogen was found to be protonated in the X-ray structure of atevirdine hydrochloride, this nitrogen may form a critical hydrogen bond with the RT enzyme. Thus optimum positioning of this nitrogen would be critical for good bioactivity. In fact, analogs of atevirdine in which the pyridine ring is replaced with a benzene ring exhibit a loss of RT inhibitory activity demonstrating the importance of the pyridine nitrogen.⁴ Extensive variation of the right-hand heterocyclic portion of the BHAP template has also demonstrated the importance of the 3-(alkylamino)pyridine moiety in obtaining good RT inhibitory activity. In other words, the mere presence of the indolyl(piperazine) portion of the template is not sufficient to produce inhibition.⁴ Therefore, the reduced activity of spiro analog **1** could also be partially accounted for by the presence of a tertiary amine at the 3-pyridine position rather than a secondary amine such as that found in atevirdine. For example, an analog containing a 3-(diethylamino)pyridyl piperazine and an unsubstituted indole moiety possessed reduced RT inhibitory activity relative to its 3-(ethylamino)pyridyl parent (60% vs 96% inhibition of RT at 100 μ M).⁴ Thus, it is probable that the rigid nature of the spirocyclic BHAP analog **1** which prevent it from exactly mimicking the enzyme bound conformation of atevirdine, and/or the presence of the less preferred tertiary amine instead of a secondary amine contribute to the lessened activity of spirocycle **1**. We look upon this preliminary result as promising, since **1** is a highly constrained system and its RT inhibitory activity indicates that we are beginning to approach the bioactive conformation of the BHAPs.

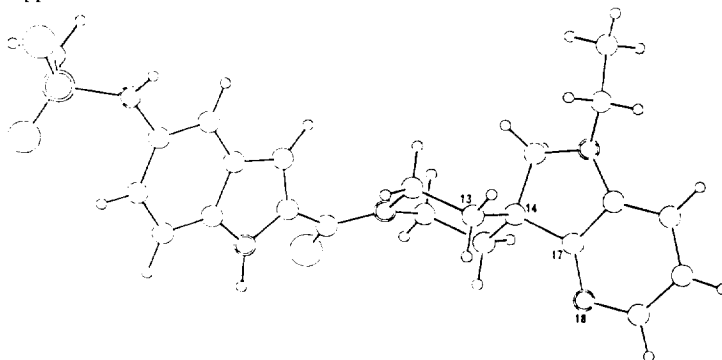


Figure 3. Energy minimized conformation of the spiro-BHAP analog **1**.^{13,14}

CONCLUSION

In this study we have prepared the conformationally constrained spiro-BHAP analog **1** based on molecular modeling and X-ray crystallography of atevirdine. This BHAP analog contains a novel spiro heterocyclic system, **6**, which has not been previously synthesized. Although **1** was less active than either atevirdine or delavirdine, the fact that it retained some RT inhibitory activity is encouraging. Therefore, it is likely that the biologically active conformation of the BHAP template is similar to the conformation induced by this spiro system. We feel this result warrants the pursuit of other related spiro-BHAP analogs.

Acknowledgment. The authors gratefully acknowledge Dr. Fritz Reusser and Ms. Irene W. Althaus for performing the biological testing of **1**.

REFERENCES and NOTES

- Romero, D. L.; Busso, M.; Tan, C.-K.; Reusser, F.; Palmer, J. R.; Poppe, S. M.; Aristoff, P. A.; Downey, K. M.; So, A. G.; Resnick, L.; Tarpley, W. G. *Proc. Natl. Acad. Sci. U.S.A.* **1991**, *88*, 8806-8810.
- Romero, D. L.; Morge, R. A.; Genin, M. J.; Biles, C.; Busso, M.; Resnick, L.; Althaus, I. W.; Reusser, F.; Thomas, R. C.; Tarpley, W. G. *J. Med. Chem.* **1993**, *36*, 1505-1508.
- Dueweke, T. J.; Poppe, S. M.; Romero, D. L.; Swaney, S. M.; So, A. G.; Downey, K. M.; Althaus, I. W.; Reusser, F.; Busso, M.; Resnick, L.; Mayers, D. L.; Lane, J.; Aristoff, P. A.; Thomas, R. C.; Tarpley, W. G. *Antimicrob. Agents Chemother.* **1993**, *37*, 1127-1131.
- Romero, D. L.; Morge, R. A.; Biles, C.; Berrios-Pena, N.; May, P. D.; Busso, M.; Palmer, J. R.; Johnson, P. D.; Smith, H. W.; Busso, M.; Tan, C.-K.; Voorman, R. L.; Reusser, F.; Althaus, I. W.; Downey, K. M.; So, A. G.; Resnick, L.; Tarpley, W. G.; Aristoff, P. A. *J. Med. Chem.* **1994**, *37*, 999-1014.
- The Cambridge Crystal Structure Database is available by license from the Cambridge Crystallographic Data Centre, Lensfield Road, Cambridge, England.
- Molecular modeling calculations on the BHAP prototype were done using the MOSAIC program, an Upjohn modified version of the MACROMODEL program.⁷
- Mohamadi, F.; Richards, N. G. J.; Guida, W. C.; Liskamp, R.; Lipton, M.; Caufield, C.; Chang, G.; Hendrickson, T.; Still, W. C. *J. Comp. Chem.* **1990**, *11*, 440-462.
- The atomic coordinates and thermal parameters are deposited at the Cambridge Crystallographic Data Centre. Experimental for the X-ray Structure Determination of atevirdine and atevirdine hydrochloride. Crystal data for atevirdine: C₂₁H₂₄N₅O₂; formula wt. = 379.5; orthorhombic; space group *Pca2₁*; Z=4; *a*=10.843(2), *b*=15.55(1), *c*=11.427(3) Å *V*=1927(1) Å³; calculated density = 1.31 g cm⁻³; absorption coefficient μ = 0.6 mm⁻¹; clear narrow plate 0.05 x 0.07 x 0.5 mm mounted on a glass fiber. Of 1380 unique reflections measured, 1153 had intensities > 3 σ . Crystal data for atevirdine hydrochloride: C₂₁H₂₅N₅O₂·HCl; Formula wt = 415.9; monoclinic; space group *P2₁/c*; Z=4; *a*=9.704(1), *b*=27.375(3), *c*=8.186(2) Å, β =108.79(2)° *V*=2058.7(1) Å³; calculated density = 1.34 g cm⁻³; absorption coefficient μ = 1.77 mm⁻¹; clear prism 0.10 x 0.15 x 0.45 mm mounted on a glass fiber. Of 3117 unique reflections measured, 2506 had intensities > 3 σ .
Final agreement parameters for atevirdine were: R=0.058 for all 1380 reflections, and 0.048 for the 1153 reflections having Fo² ≥ 3 σ ; standard deviation of fit = 3.4. Final population factors for alternate ethyl carbon positions were 58% and 42%. There is an intramolecular hydrogen bond between the NH of the ortho pyridine substituent and the piperazine nitrogen, (N-N distance: 2.732(8) Å), and an intermolecular hydrogen bond between the NH of the indole and the carbonyl oxygen in the symmetry related molecule at *1-x, 2-y, z-0.5*; (N-O distance: 2.889(5) Å).
Final agreement parameters for atevirdine hydrochloride were: R=0.083 for all 3117 reflections, and 0.073 for the 2506 reflections having Fo² ≥ 3 σ ; standard deviation of fit=3.1. There are intramolecular hydrogen bonds between the NH of the ortho pyridine substituent and the piperazine nitrogen, (N-N distance: 2.801(5) Å), and between the NH of the indole and the carbonyl oxygen (N-O distance 2.584(4) Å). In addition the chlorine accepts hydrogens from the protonated pyridine

nitrogen in the same symmetry, from the pyridine substituent NH in the molecule related by a translation in *z*, and from the indole NH in the molecule related by the *c* glide (N-Cl distances 3.105(4), 3.329(3), and 3.276(3), respectively).

Intensity data for both structures were measured at low temperature, -120°C, on a Siemens P21 diffractometer, using $\theta/2\theta$ scans with scan widths $\geq 3.4^\circ$ and a scan rate of $2^\circ/\text{min}$. (atevirdine), and $4^\circ/\text{min}$. (atevirdine hydrochloride). Graphite monochromatized CuK α radiation was used, ($\lambda(\text{CuK}\alpha) = 1.5418\text{\AA}$), with maximum $2\theta = 135.0^\circ$. The total time spent counting background, half at each end of the scan, was equal to the time spent scanning. Ten reflections periodically monitored showed no trend towards deterioration; $\sigma^2(I)$ was approximated by $\sigma^2(I)$ from counting statistics + $(0.01I)^2$ (atevirdine), or $(0.05I)^2$ (atevirdine hydrochloride), where the coefficient of *I* was calculated from the variations in intensities of the monitored reflections. Cell parameters were determined by least squares fit of $K\alpha_1$ 2θ values ($\lambda K\alpha_1 = 1.5402$) for 25 high 2θ reflections.¹⁷ An Lp correction appropriate for a monochromator with 50% perfect character was applied.

Both structures were solved by direct methods; atevirdine was solved using MULTAN80;¹⁸ DIREC¹⁹ was used to solve atevirdine hydrochloride. Least squares refinements included coordinates for all atoms and anisotropic thermal parameters for nonhydrogen atoms, with the exception that the disordered ethyl carbons in atevirdine were kept isotropic and hydrogens on those atoms were not included. Temperature factors for hydrogens were assigned as one-half unit higher than the equivalent isotropic temperature factors for the attached carbon. The function minimized in the refinement was $\Sigma w(F_o^2 - F_c^2)^2$, where weights *w* were $1/\sigma^2(F_o^2)$. In the final cycles all shifts were $\leq 0.3\sigma$. Atomic form factors were from Doyle and Turner,²⁰ and, for hydrogen, from Stewart, Davidson and Simpson.²¹ The CRYM system of computer programs was used.¹⁹

9. Eisleb, O. *Chem. Ber.* **1941**, *74*, 1433.
10. Ong, H.H.; Profitt, J. A.; Fortunato, J.; Glamkowski, E. J.; Ellis, D. B.; Geyer, H. M.; Wilker, J. C.; Burghard, H. *J. Med. Chem.* **1983**, *26*, 981.
11. Goehring, R. R.; Sachdeva, Y. P.; Pisipati, J. S.; Sleevi, M. C.; Wolfe, J. F. *J. Am. Chem. Soc.* **1985**, *107*, 435-443.
12. Representative physical data for **1** crystallized from MeOH/Et₂O, mp 240-241 °C; ¹H NMR (300 MHz, CDCl₃) δ 1.14 (t, *J* = 7.12 Hz, 3 H), 1.70-1.85 (m, 2 H), 2.05-2.20 (m, 2 H), 2.90 (s, 3 H), 3.13 (q, *J* = 7.22 Hz, 2 H), 3.30 (s, 2 H), 3.55 (br, 2 H), 4.45-4.55 (m, 2 H), 6.59-6.67 (m, 3 H), 6.90 (dd, *J* = 5.0, 8.0 Hz, 1 H), 7.08 (dd, *J* = 2.1, 8.7 Hz, 1 H), 7.34 (d, *J* = 8.7 Hz, 1 H), 7.50 (s, 1 H), 7.75 (dd, *J* = 1.2, 5.0 Hz, 1 H), 9.40 (s, 1 H). ¹³C NMR (75 MHz, CDCl₃) δ 11.28, 19.52, 34.55, 38.77, 42.26, 43.15, 64.18, 104.84, 112.24, 112.58, 116.46, 120.61, 122.56, 127.89, 129.64, 130.97, 133.97, 137.35, 145.00, 161.91. HRMS Calcd. for C₂₃H₂₇N₅O₃S: 453.1834. Found: 453.1830.
13. This assay has been described by us previously in references 1-4.
14. In an analogous HIV-1 RT assay system, **1** inhibited the enzyme 45% at 50 μM , compared to delavirdine which inhibited 99% at 50 μM .
15. Energy minimization of the spiro-BHAP analog **1** were done using the molecular mechanics program CONFOS developed at The Upjohn Company by David J. Duchamp. The development and parameterization of the force-field used is described in reference 14.
16. Duchamp, D. J.; Pschigoda, L. M.; Chidester, C. G. *Molecular Mechanics, Crystallography, and Drug Research, Molecular Structure, Chemical Reactivity and Biological Activity*, Stezowski, J. J., Ed.; Oxford University Press: New York, **1988**, 34-39.
17. Duchamp, D.J. *Newer Computing Techniques for Molecular Structure Studies by X-Ray Crystallography. ACS Symp. Ser.*, **1977**, No. 46, 98-121.
18. Main, P.; Fiske, S.J.; Hull, S.E.; Lessinger, L.; Germain, G.; Declercq, J.P. & Woolfson, M.M. (1980). *MULTAN80. A System of Computer Programs for the Automatic Solution of Crystal Structures from X-ray Diffraction Data*. Univs. of York, England, and Louvain, Belgium.
19. Duchamp, D.J., 1984, DIREC, a direct methods program for solving crystal structures, and CRYM, a system of crystallographic programs. The Upjohn Company, Kalamazoo, MI.
20. Doyle, P.A., & Turner, P.S. Relativistic Hartree-Fock X-ray and Electron Scattering Factors. *Acta Crystallogr.* **1968**, *A24*, 390-397.
21. Stewart, R.F., Davidson, E.R., & Simpson, W.T. Coherent X-ray Scattering for the Hydrogen Atom in the Hydrogen Molecule. *J. Chem. Phys.*, **1965**, *42*, 3175-3187.